Remote Sensing of Environment 216 (2018) 201–211

Contents lists available at ScienceDirect

Remote Sensing of Environment

journal homepage: www.elsevier.com/locate/rse

Mapping continuous fields of tree and shrub cover across the Gran Chaco using Landsat 8 and Sentinel-1 data

Matthias Baumann[a,*], Christian Levers[a], Leandro Macchi[a,b], Hendrik Bluhm[a], Björn Waske[c], Nestor Ignacio Gasparri[b,d], Tobias Kuemmerle[a,d]

[a] Geography Department, Humboldt-Universität zu Berlin, Unter den Linden 6, 10099 Berlin, Germany
[b] CONICET, Instituto de Ecología Regional (IER), Universidad Nacional de Tucumán, CC:34, CP 4107 Yerba Buena, Tucumán, Argentina
[c] Institute of Geographical Sciences, Freie Universität Berlin, Malteserstr. 74 - 100, Berlin 12249, Germany
[d] Integrative Research Institute on Transformations of Human-Environment Systems (IRI THESys), Humboldt-Universität zu Berlin, Unter den Linden 6, 10099 Berlin, Germany

ARTICLE INFO

Keywords:
Gradient Boosting Regression
Savannas
Tropical dry forests
Canopy structure
Forest degradation
Essential Biodiversity Variables (EBVs)
Vegetation Continuous Fields (VCFs)
Sensor fusion

ABSTRACT

Tropical dry forests and savannas provide important ecosystem services and harbor high biodiversity, yet are globally under pressure from land-use change. Mapping changes in the condition of dry forests and savannas is therefore critical. This can be challenging given that these ecosystems are characterized by continuous gradients of tree and shrub cover, resulting in considerable structural complexity. We developed a novel approach to map, separately, continuous fields of tree cover and shrub cover across the South American Gran Chaco (1,100,000 km^2), making full use of the Landsat-8 optical and Sentinel-1 synthetic aperture radar (SAR) image archives. We gathered a large training dataset digitized from very-high resolution imagery and used a gradient-boosting framework to model continuous fields of tree cover and shrub cover at 30-m resolution. Our regression models had high to moderate predictive power (85.5% for tree cover, and 68.5% for shrub cover) and resulted in reliable tree and shrub cover maps (mean squared error of 4.4% and 6.4% for tree- and shrub cover respectively). Models jointly using optical and SAR imagery performed substantially better than models using single-sensor imagery, and model predictors differed strongly in some regions, especially in areas of dense vegetation cover. Mapping tree and shrub cover separately allowed identifying distinct vegetation formations, with shrub-dominated systems mainly in the very dry Chaco, woodlands with large trees mainly in the dry Chaco, and tree-dominated savannas in the wet Chaco. Our tree and shrub cover layers also revealed considerable edge effects in terms of woody cover away from agricultural fields (edge effects extending about 2 km), smallholder ranches (about 1.2 km), and roads and railways (about 1.4 and 0.9 km, respectively). Our analyses highlight both the substantial footprint of land-use on remaining natural vegetation in the Chaco, and the potential of multi-sensoral approaches to monitor forest degradation. More broadly, our approach shows that mapping canopy structure and distinct layers of woody vegetation in dry forest and savannas is possible across large areas, and highlights the value of the growing Landsat and Sentinel archives for doing so.

1. Introduction

Tropical dry forests and savannas cover about 20% of the Earth's surface, account for about 30% of the primary production of all terrestrial vegetation (Grace et al., 2006), harbor high biodiversity (Mayle et al., 2007), and provide many important ecosystem services (Abreu et al., 2017; Lehmann, 2010; Murphy et al., 2016; Parr et al., 2014). However, dry forests and savannas are under increasing pressure from agricultural expansion and intensification (Espirito-Santos et al., 2016; Kaya et al., 2018; Klink and Machado, 2005), leading to major carbon emissions (Chen et al., 2018; González-Roglich and Swenson, 2016; Lucas et al., 2011), and biodiversity losses (Ratter et al., 1997). Monitoring the condition of dry forest and savannas is therefore important.

This is challenging given the nature of these ecosystems, characterized by continuous gradients of woody and grass cover (House et al., 2003; Sankaran et al., 2008). These ecosystems can contain a wide variety of canopy types, including woodlands dominated by smaller trees and shrubs (House et al., 2003), woodlands with interspersed larger trees, and savannas dominated by grassland and scattered palm trees (Bucher, 1982), or shrublands (Archer et al., 1995;

* Corresponding author.
E-mail address: matthias.baumann@hu-berlin.de (M. Baumann).

https://doi.org/10.1016/j.rse.2018.06.044
Received 26 March 2018; Received in revised form 22 June 2018; Accepted 27 June 2018

Asner et al., 2003; Roques et al., 2001). This complexity in vegetation types arises from heterogeneous soils, climate conditions and, importantly, land use (Morgan et al., 2007; Polley et al., 1997). For example, fire suppression in savannas often results in increasing shrub cover and declining grassy vegetation (Archibald et al., 2005; Moreira, 2000). Similarly, logging and firewood collection lead to a loss of large trees (Gillespie et al., 2000), and grazing by cattle or goats might reduce or increase shrub cover (Stern et al., 2002). Monitoring gradients of woody vegetation, and stratifying woody cover into tree and shrub components, is therefore important for better understanding dry forest and savanna structure, composition, and functioning.

Remote sensing is a key technology to do so, and regression-based approaches to derive continuous fields of woody vegetation (Hansen et al., 2003; Hayes et al., 2008; Pengra et al., 2015) are particularly promising. Approaches to map fractions of woody cover were originally introduced to overcome limitations due to relative coarse resolution of sensors such as the Advanced Very High Resolution Radiometer (AVHRR) (Defries et al., 2000; Hansen and DeFries, 2004; Hansen et al., 2003) or the Moderate Resolution Image Spectroradiometer (MODIS) (Hansen et al., 2006; Hansen et al., 2003). While this has increased our understanding of the global distribution of woody cover substantially, broad-scale products are typically too coarse to provide reliable estimates for dry forests and savannas. With the opening of the Landsat archives (Wulder et al., 2012) mapping continuous fields of woody cover across local (Gessner et al., 2013; Johansen and Phinn, 2006), regional (Higginbottom et al., 2018; Schwieder et al., 2016), and continental extents (Hansen et al., 2011; Hansen et al., 2013) has become possible, representing a step change in our understanding of woody cover gradients. Yet, current broad-scale products still have low accuracy in dry forests and savannas (Brandt et al., 2016; Hansen et al., 2013; Sexton et al., 2013; Tian et al., 2016).

Existing approaches also typically do not allow separating between tree and shrub cover which would be important to assess dry forest and savanna complexity. Tree and shrub cover maps are potentially highly useful for land-use and conservation planning in savannas and dry forests, given that these systems are lost rapidly in many places, yet remain often unmapped (de Carvalho and Mustin, 2017). Mapping tree and shrub cover separately would also allow assessing the role of land use in shaping natural vegetation, moving beyond assessing full conversion only towards better capturing processes of woodland degradation. For example, grazing impacts are often highest close to a farm but decrease with larger distances (Macchi and Grau, 2012), and extractive activities such as logging are often highest close to infrastructure such as roads or railways (Chomitz and Gray, 1995). The spatial footprint of such land-use processes, however, is often unknown.

A promising avenue for stratifying woody cover into tree and shrub constituents is to combine Landsat imagery with synthetic aperture radar (SAR) imagery, as these data are highly complementary (Joshi et al., 2016). For example, optical data are powerful for mapping large trees, particularly when the phenology of vegetation is considered (Melaas et al., 2016), but have limited capabilities in identifying scattered woody vegetation. Contrary, SAR signals respond well to the density and size of scattering elements and are therefore potentially powerful to map sparser woody vegetation (Durigan and Ratter, 2006; Mitchard et al., 2011; Ryan et al., 2012; Santos et al., 2002). A number of studies have attempted to map savannas and dry forests by combining these data, for example in the Cerrado (Carreiras et al., 2017), in the South Africa-Mozambique border region (Naidoo et al., 2016), or in Bolivia (Reiche et al., 2018). Yet, these studies either mapped small regions only, classified savannas and dry forests into broad categories, or did not distinguish between trees and shrubs. A new generation of sensors now provides potentials for an improved mapping of dry forest and savanna vegetation. Landsat 8, operational since 2013, provides global coverage of high-resolution optical data at unprecedented radiometric resolution (Irons et al., 2012; Roy et al., 2014). Likewise, the Sentinel-1 sensors (since 2014) provide consistent C-band SAR data at high temporal and spatial resolution. Combining these data should provide tremendous potential for dry forest and savanna mapping, but to our knowledge, no study has attempted to do so across larger areas.

We focused on the Gran Chaco, a 1.1 million km^2 dry forest region in South America characterized by strong gradients in woody vegetation cover. The Gran Chaco contains dense and tall dry forests, palm savannas, open grasslands, and shrublands (Bucher, 1982), and is also a global hotspot of land-use change, with many land-use practices affecting the extent and composition of woody vegetation in the landscape (Grau et al., 2008; le Polain de Waroux et al., 2017). Yet, spatial patterns of woody cover and composition remain unclear, or are only available for smaller study regions (Cabido et al., 2018). Our overarching goal was thus to develop a methodology to use Landsat-8 and Sentinel-1 data to characterize woody vegetation across the Chaco. Specifically, our objectives were:

1. to map continuous fields of tree and shrub cover across the entire Chaco,
2. to assess whether the joint use of Landsat-8 and Sentinel-1 data improves the mapping of these woody cover components,
3. to map major vegetation types of dry forests and savannas across the Chaco, and
4. to assess the relationship of tree and shrub cover and a suite of environmental and socio-economic variables.

2. Methods

2.1. Study area

Our study area encompassed the entire Gran Chaco in South, stretching across Argentina, Bolivia and Paraguay, as well as into Brazil (Fig. 1, inlet). The Chaco is characterized by a marked dry season from May to September, with mean monthly temperatures of up to 29 °C, and a rainfall gradient between 1200 mm and 450 mm in the center, which results in substantially vegetation heterogeneity across the Chaco. In the west, medium-tall xerophyllous forests are dominant, with trees about 12 m high and sometimes reaching 18 m (Bucher, 1982). The eastern Chaco represents the wettest part, with widespread wetlands. The dominant vegetation types are wet savannas consisting of a mosaic of dense or open woodland patches, intermixed with grasslands. The woodland patches are occupied by subtropical semi-deciduous forests, with some trees reaching 25–30 m (Bucher, 1982), and gallery forest, mainly along the Paraguay and Parana rivers. Two semi-deciduous (*schinopsis balansae* and *astronium balansae*) and one evergreen species (*aspidosperma quebracho blanco*) are dominant here. The central Chaco is an ecotone between the eastern and the western Chaco, and dominated by xerophyllous subtropical forests with quebrachos (*Schinopsis quebrachos colorados*, *S. lorentzii*, and *Aspidosperma quebracho*), but also with grasslands and savannas dominated by wire grasses (*Elionorus muticus*) (Bucher, 1982; Cabrera, 1976). The driest section is the very dry Chaco in the south. Here, large trees are almost absent and grassland-shrub savannas (mostly *spartina argentinensis* and *Elionurus muticus*) with scattered low trees (mainly *proposes algarrobilla*) dominate (Bucher, 1982).

The Chaco is also a global hotspot of deforestation (Baumann et al., 2017b; Graesser et al., 2015; Kuemmerle et al., 2017), with various land-use actors affecting tree- and shrub-cover differently. Industrialized agribusinesses are now common in the Chaco, producing cattle and soybean (Baumann et al., 2016; Piquer-Rodríguez et al., 2018). In the case of cropping, no woody vegetation (i.e., no trees and shrubs) remains on the fields, and massive pesticide applications and run-away agricultural fires affect the surrounding woody vegetation. Pastures are traditionally also cleared completely of all trees and shrubs, but long-term grazing results in shrub encroachment. In recent years, so-called silvipastures are increasingly common, as the Argentine Ley de Proteccion Ambiental de Bosques Nativos (2007) requires

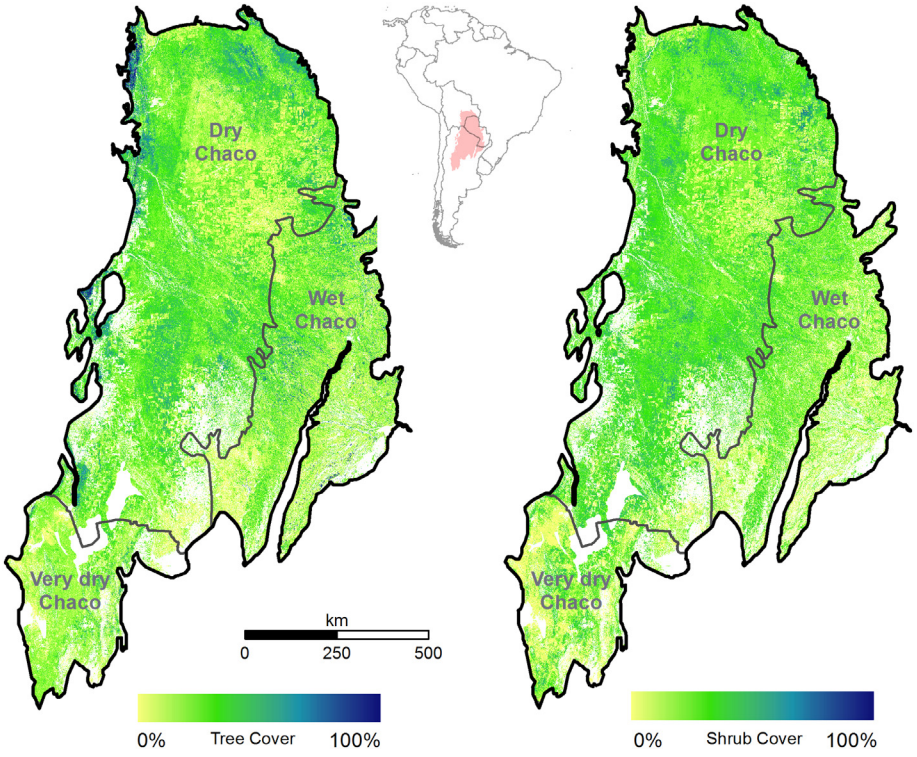

Fig. 1. Mapping results for fractional tree cover (TC) and fractional shrub cover (SC). We masked out all areas without any vegetation (e.g., salt planes, croplands, urban areas) and set the respective TC and SC values to zero, based on a previous land-cover classification (Baumann et al., 2017a). The inset map shows the location of the Gran Chaco in South America.

ranchers to retain a proportion of the woody cover on pastures (Ceddia and Zepharovich, 2017); typically the large trees (~5%–30% canopy cover), while smaller trees and shrubs are removed (Rejžek et al., 2017). In addition, charcoal production and logging focusses on removing large and valuable trees, dominantly using selective cutting leaving woodlands dominated by smaller trees and shrubs (Rueda et al., 2015). Lastly, smallholders, so-called puesteros, use woodlands for cattle, sheep and goat grazing, and for extracting fuel and construction wood. This results in a modified canopy structure with lower tree cover and sometimes higher shrub cover around smallholder farms (Grau et al., 2008; Macchi et al., 2013).

2.2. Compositing of Landsat and Sentinel-1 data

We based our analysis on image composite metrics, which we generated using all available Landsat 8 and Sentinel-1 images. Image composite metrics are gap-free mosaics based on all available images, in case of optical data cloud-free observations, within a user-defined study region and period (Griffiths et al., 2013; Potapov et al., 2015; Roy et al., 2010). Compared to traditional, single-image approaches they are advantageous for at least two reasons. On one hand, in the case of optical data, using many or all available images minimizes limitations due to clouds or cloud shadows. On the other hand, image composite metrics represent aggregated measures of the reflectance and the structure of the surface (e.g., mean reflectance or backscatter over a year) and therefore are able to capture phenology and climate effects on vegetation (Bleyhl et al., 2017; Griffiths et al., 2014). To make use of these advantages, we downloaded all available images (1994 Landsat images and 1067 Sentinel-1 available images) for the Chaco for the year 2015.

Landsat imagery came from the United States Geological Survey (USGS, 2015) in terrain-corrected quality (L1T), as surface reflectance values generated though LEDAPS (Masek et al., 2006), and with cloud masks based on Fmask (Zhu and Woodcock, 2012) and therefore did not require further pre-processing. Contrary, the Sentinel-1 data required substantial pre-processing for which we employed the python-implementation *snappy* of the Sentinel Application Platform (SNAP). We downloaded all Sentinel-1 imagery as dual-polarized (i.e., vertical-vertical (VV) and vertical-horizontal (VH)) data in Interferometric Wide-Swath Mode (IW) and Ground-Range Detected High Resolution (GRDH) at a spatial resolution of 10 m. First, we applied an orbit file and a radiometric calibration. Second, we performed a Range-Doppler Terrain-Correction, using 30 m Shuttle Radar Topography Mission (SRTM) data (Ottinger et al., 2017). Last, we matched the 10 m Sentinel-1 resolution to our 30 m Landsat grid by averaging all Sentinel-1 pixels within a Landsat grid cell, thus reducing the SAR inherent speckle without applying an individual speckle filter.

After pre-processing, we calculated image composite metrics, purposefully choosing metrics least affected by outliers (e.g., due to errors in cloud masks or due to differing image availability). For the Landsat imagery, we calculated the per-band mean, median and 75th percentile reflectance. For the Sentinel-1 imagery, we calculated the per-polarization mean, median and 75th percentile σ_0 values. We stacked the metrics into three input datasets for our analyses: (1) *Landsat only* consisting of 18 bands (three metrics for six spectral bands); (2) *Sentinel-1 only* consisting of six bands (three metrics for two polarizations); and (3) *Landsat-Sentinel-1 combined* consisting of 24 bands.

2.3. Mapping fractional tree- and shrub cover using Gradient Boosting Regression (GBR)

We used our image composite metrics together with an extensive training dataset within a Gradient Boosting Regression (GBR) framework to derive continuous fields of tree cover and shrub cover. Tree cover here refers to large trees with a height of at least 10 m height. Contrary, shrub cover refers to larger and smaller shrubs but also smaller trees with a height of < 10 m, and we made this distinction based on existing field inventory plots from our own previous work (Gasparri et al., 2008).

Our training dataset consisted of a stratified random sample of hand-digitized proportions of tree and shrub cover per-pixel based on high-resolution imagery in Google Earth. To derive a representative sample of different degrees of tree and shrub cover, we relied on a previous map (Baumann et al., 2017a), which contains six major land-cover types. We sampled 100 sampling plots of 900 m^2 (i.e., one

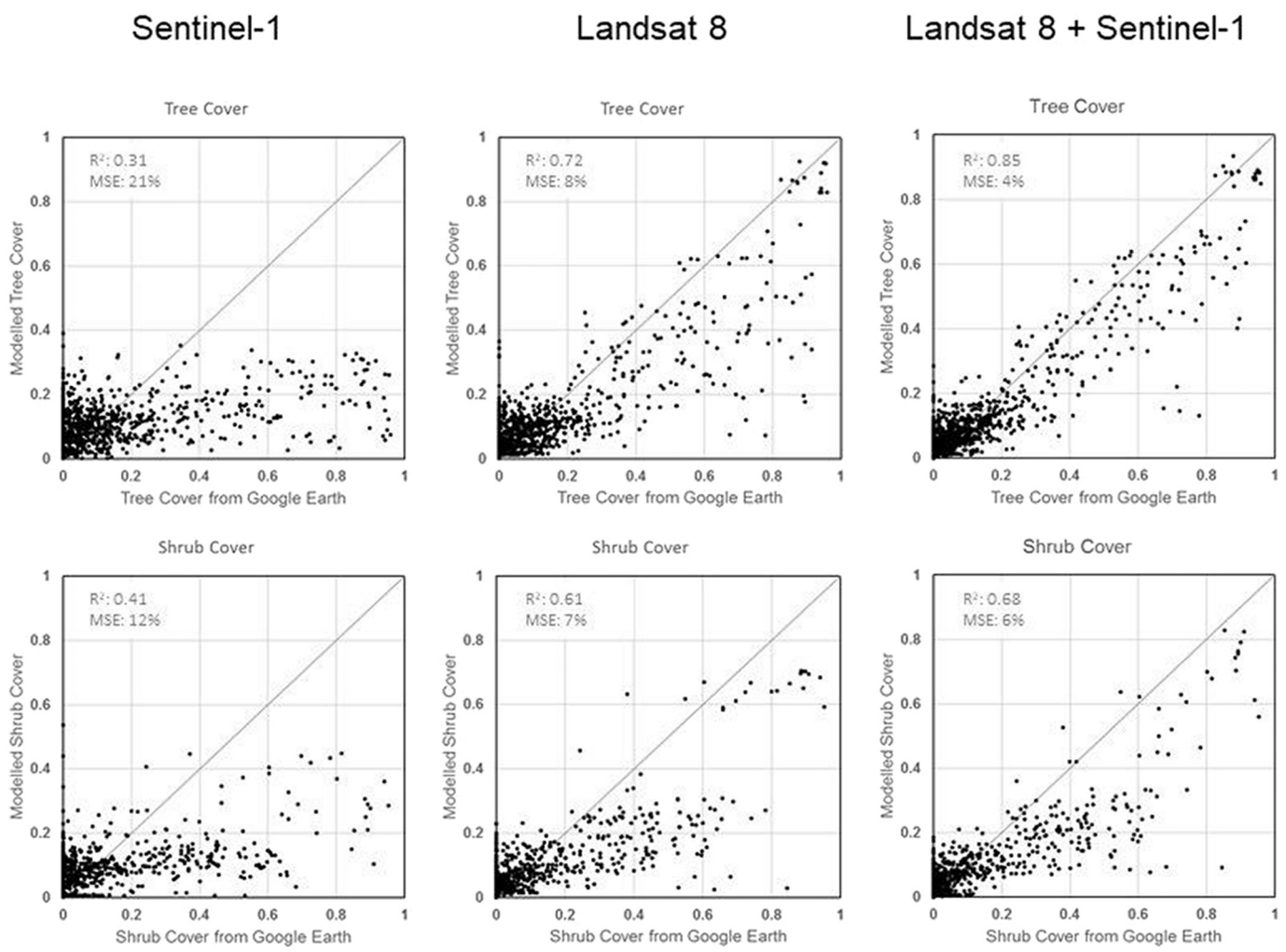

Fig. 2. Cross-validated model results of the Gradient Boosting Regression (GBR) when using Sentinel-1 data (left column) or Landsat 8 data (middle column) only, and using Sentinel-1 and Landsat 8 data together (right column). Plotted are the shrub cover from Google Earth (i.e., the digitized values) vs. modelled values for fractional tree cover (top row) and fractional shrub cover (bottom row).

Table 1
Mean and standard deviation of tree-and shrub-cover across the Chaco and its sub regions (i.e., wet, dry and very dry Chaco), depending on the satellite imagery used.

Region	Sensor(s)	Mean tree cover [%]	Mean shrub cover [%]
Chaco	Landsat 8 + Sentinel-1	10.6 (8.9)	6.5 (4.4)
	Landsat 8	9.3 (12.1)	5.8 (6.0)
	Sentinel-1	8.3 (6.85)	6.0 (6.2)
Wet Chaco	Landsat 8 + Sentinel-1	9.9 (8.3)	4.8 (3.2)
	Landsat 8	9.48 (12.83)	4.64 (4.95)
	Sentinel-1	7.29 (6.1)	4.94 (5.36)
Dry Chaco	Landsat 8 + Sentinel-1	11.7 (9.5)	7.8 (4.6)
	Landsat 8	10.55 (12.46)	6.83 (6.57)
	Sentinel-1	9.66 (7.11)	7.32 (6.47)
Very dry Chaco	Landsat 8 + Sentinel-1	6.5 (5.5)	4.2 (3.6)
	Landsat 8	3.41 (5.71)	3.34 (3.93)
	Sentinel-1	3.7 (4.32)	2.07 (3.67)

Landsat pixel) with a minimum distance of 900 m (i.e., 30 Landsat pixels) into each class, except for dense forest and palm savannas, into which we sampled 200 plots given the importance of these categories for our study. Hence, our sample consisted of a total of 1000 independent, randomly selected plots. For 356 sample plots (35.6%), high-resolution imagery in Google Earth (i.e., Quickbird resolution of 0.65 m or finer) was available and we discarded all other plots. We digitized tree and shrub cover in a window of 3 × 3 Landsat pixels (i.e., 900 m × 900 m = 8100 m^2) to account for possible misregistration of the Google Earth imagery (Potere, 2008), and calculated average area fractions that we assigned to the central pixel (i.e., our sample plot).

We then used these per-pixel fractions as input for a GBR model to derive continuous fields of tree and shrub cover. GBR is a machine learning algorithm which makes predictions based on ensembles of individual decision trees (Elith et al., 2008). Contrary to random forests or other bagging algorithms, GBR grows new trees based on the errors (or residuals) of the previously fitted trees (Friedman, 2001). Each tree thereby has a weight, and the final GBR model is then the average of all weighted trees. GBR are able to handle heterogeneous data efficiently, to identify non-linear responses, and to account for feature interactions (Ridgeway, 2007). We followed Hastie et al. (2009) to tune five parameters: (1) the learning rate that shrinks the contribution of each tree; (2) the number of estimators that sets the number of boosting stages; (3) the maximum depth that limits the number of nodes in a tree; (4) the minimum number of observations at a leaf node; and (5) the number of features required for a tree to be considered when looking for the best split. We systematically tested a wide range of parameter combinations by fitting a GBR model for each parameter combination and evaluating these models using 10-fold cross-validation. Because our ground data are independent from each other (random sampling scheme, minimum distance of 900 m between plots) this results in a reliable estimation of

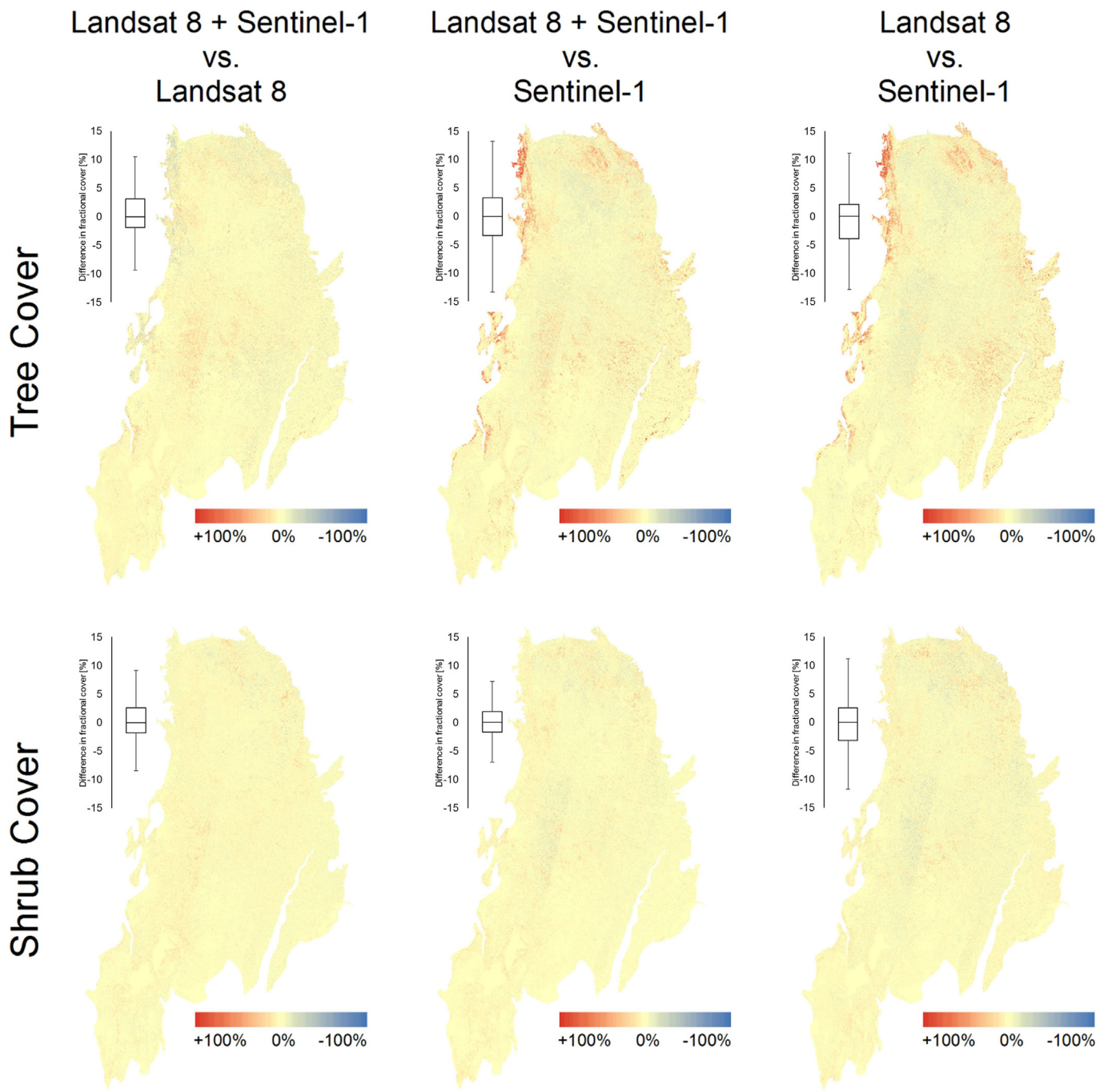

Fig. 3. Differences in tree and shrub cover between the three input datasets. Positive differences indicate higher estimates in the first-named data product (e.g., Landsat 8 + Sentinel-1 in the upper left map) whereas negative differences indicate higher values in the second-named product (e.g., Landsat 8 in that case). The boxplots represent the distribution of values across the Chaco.

model fit and accuracy. We then selected the parameter combination with the lowest mean-squared error (MSE), and re-fitted this model using all available training data. This means our error estimates are a conservative measure of our final model (and map accuracy), which was based on all training data (Pedregosa et al., 2011). Lastly, we plotted the observed vs. predicted values of tree and shrub cover, and calculated Pearson's correlation coefficient. We repeated this procedure for each of our three input datasets (i.e., Landsat, Sentinel-1, and combination thereof).

We then predicted tree and shrub cover across the entire Chaco by applying the respective model to the entire input dataset. Once tree and shrub cover maps were available for each input dataset, we calculating difference maps for all combinations (i.e., tree and shrub cover for Landsat/Sentinel vs. Landsat-only; Landsat/Sentinel vs. Sentinel-only; Landsat-only vs. Sentinel-only). We summarized mean and standard deviation differences of tree and shrub cover for the dry, very dry and wet Chaco for each map.

2.4. Spatial patterns of tree and shrub cover in the Chaco

To analyze spatial patterns of tree and shrub across the Chaco landscape, we first calculated the global bivariate to quantify the spatial autocorrelation between tree and shrub cover (Anselin et al., 2006). Second, we calculated the bivariate local indicator of spatial association

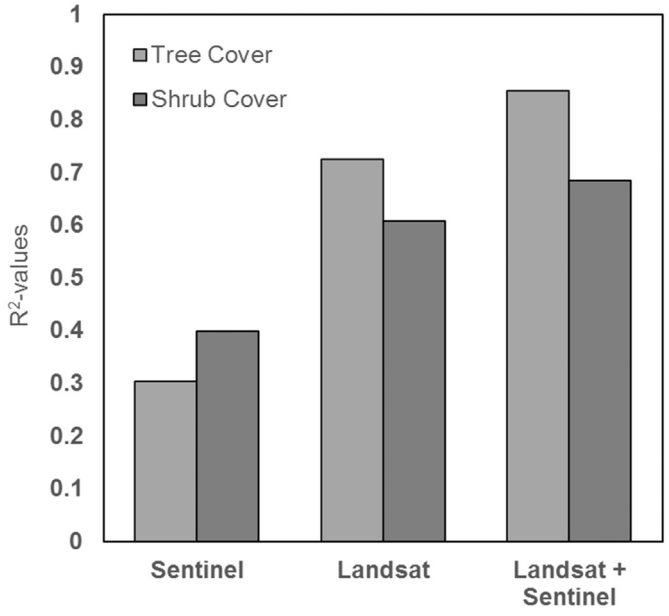

Fig. 4. Overall model performances of the Gradient Boosting Regression for fractional tree cover and shrub cover.

(bLISA) that quantifies the association of tree and shrub cover in a spatially explicit way (Anselin et al., 2006). Specifically, bLISA tests if the value of a variable in a given location is more similar to the average of a second variable in neighboring locations compared to the case under spatial randomness (Anselin, 1995). In our case, the bLISA metric resulted in spatial *clusters* of tree and shrub cover (i.e., high tree cover surrounded by high shrub cover, or low tree cover surrounded by low shrub cover) or in spatial *outliers* (i.e., high tree cover surrounded by low shrub cover, or low tree cover surrounded by high shrub cover). We identified statistically significant spatial clusters or outliers using a Monto-Carlo randomization with 999 permutations and a significance level of $p = 0.05$ (Anselin et al., 2006).

We also evaluated our woody vegetation components in relation to environmental and land-use factors that might influence tree and shrub cover in the Chaco. In terms of environmental variables, we compared tree and shrub cover to a cation exchange capacity (CEC) layer from the ISRIC soil database (ISRIC - World Soil Information, 2013), in which higher CEC indicates higher soil fertility. Likewise, we compared our tree and shrub cover values to the Hargreaves' Climatic Moisture Deficit (CMD) from the ClimateSA dataset (Hamann et al., 2013). For both variables, we compared tree and shrub cover to them at 10,000 randomly sampled points across our study region.

In terms of land-use variables, we assessed changes in tree and shrub cover in relation to the Euclidian distance to croplands (Baumann et al., 2017a). Second, we assessed tree and shrub cover changes away from homesteads (*puestos*), using a puesto dataset for northern Argentina, where they are widespread (Grau et al., 2008). Third, we assessed tree and shrub cover away from roads and railways. For each of these variables, we calculated 100-m buffers up to a distance of 6 km, randomly sampled 50 points in each buffer zone (10 points only in the two smallest buffers) and calculated mean tree and shrub cover per buffer zone.

3. Results

Our GBR models showed high performance. The goodness-of-fit of our best model was higher for tree cover (R^2 of 0.85, MSE of 4%) compared to shrub cover (R^2 of 0.68, MSE of 6%, Fig. 4). Generally, our models underestimated both tree and shrub cover, but particularly shrub cover, in the mid-value range (between 20% and 60% tree and shrub cover, respectively, Fig. 2). The GBR models showed the highest performances when using data from Landsat and Sentinel-1 together compared to Landsat only (R^2 values of 0.72 and 0.61 and MSE of 8% and 7% for tree and shrub cover, respectively) and Sentinel-1 only (R^2 values of 0.31 and 0.41, MSE of 21% and 12% for tree and shrub cover, respectively, Fig. 4).

Tree and shrub cover varied across our study region. According to our best models (i.e., the ones using Landsat 8 and Sentinel-1 data), mean (M) tree and shrub cover across the Chaco were 10.6% (standard deviation (SD): 8.9%) and 6.5% (SD: 4.4%), and maximum (Max) tree and shrub cover were 89.0% and 46.2%, respectively. Tree cover was highest in the dry Chaco (M: 11.7%, SD: 9.5%, Max: 88%), followed by the wet Chaco (M: 9.9%, SD: 8.3%, Max: 88.5%), and was lowest in the very dry Chaco (M: 6.5%, SD: 5.5%, Max: 89%). Likewise, shrub cover was highest in the dry Chaco (M: 7.8%, SD: 4.6%, Max: 46.2%) followed by the wet Chaco (M: 4.8%, SD: 3.2%, Max: 35%) and the very dry Chaco (M: 4.2%, SD: 3.6%, Max: 26.25%) (Table 1).

Differences among the tree and shrub cover map were generally relatively little, as highlighted by the distribution of differences among the different map products (Table 1). Differences were similar for tree cover (around 9% on average) and shrub cover, though slightly smaller for the latter (around 6%, Table 1). Projecting these models to the entire revealed some strong artefacts in the form of striping (as a result of image availability, Fig. 3). These artefacts were most visible for shrub cover and in areas where Sentinel-1 data were scarce (e.g., in the center of our study area, Fig. 3). High differences also occurred in ecotone areas to the Yungas biome (e.g., north-west of our study area) and for wetland areas (e.g. north-east of our study region).

The global bivariate Moran's I between tree and shrub cover was 0.36, indicating a moderate spatial association (i.e., clustering) between tree and shrub cover. Local autocorrelation between tree and shrub cover was statistically significant in 73.5% of the study area, and the resulting spatial clusters/outliers occupied 23.5% (High tree cover and high shrub cover), 35% (low tree cover and low shrub cover), 10% (low tree cover and high shrub cover), and 5% (high tree cover and low shrub cover) of the study area (Fig. 5). Areas with high tree cover and high shrub cover are likely those forests of particularly conservation value (e.g., less degraded, highest carbon stocks). When comparing these areas to the protected area network of the Chaco, we found that only 12% of these areas fall inside these protected areas.

Relating our tree and shrub cover to environmental and land-use factors revealed distinct patterns. In case of environmental variables, we found that tree and shrub cover values were similar within similar conditions, but sharply decreased outside this domain. For example, in case of cation exchange capacity, we found constant values for tree and shrub cover between 15 and 21 $cmol_c/kg$, but a sharp decline in tree and shrub cover for values below 15 and higher 21 $cmol_c/kg$ (Fig. 6A). In case of the CMD, we found that tree cover decreased with increasing CMD, but was higher at very high CMD values (Fig. 6B).

Comparing tree and shrub cover values to land-use factors, revealed that each factor influenced tree and shrub cover values distinctly. Tree and shrub cover were both lowest (~1%) in the immediate surroundings of puestos, and increased away from them up until a certain distance at which they leveled off (Fig. 6D). For shrub cover this distance was at around ~700 m to the puesto (10%), compared to ~1.2 km for tree cover (15%). For croplands, the pattern was similar: tree cover leveled off after ~2 km (tree cover of 15%), whereas for shrub cover this point was reached earlier (i.e., ~600 m, shrub cover of ~10%, Fig. 6C). In case of distance to roads and railways, tree cover was lower closer to roads and railways (10–12% for roads, and < 10% for railways, respectively), and then increased, but we did not find the same pattern for shrub cover (Fig. 6E, F).

4. Discussion

Land use exerts strong pressure on the world's tropical dry forests

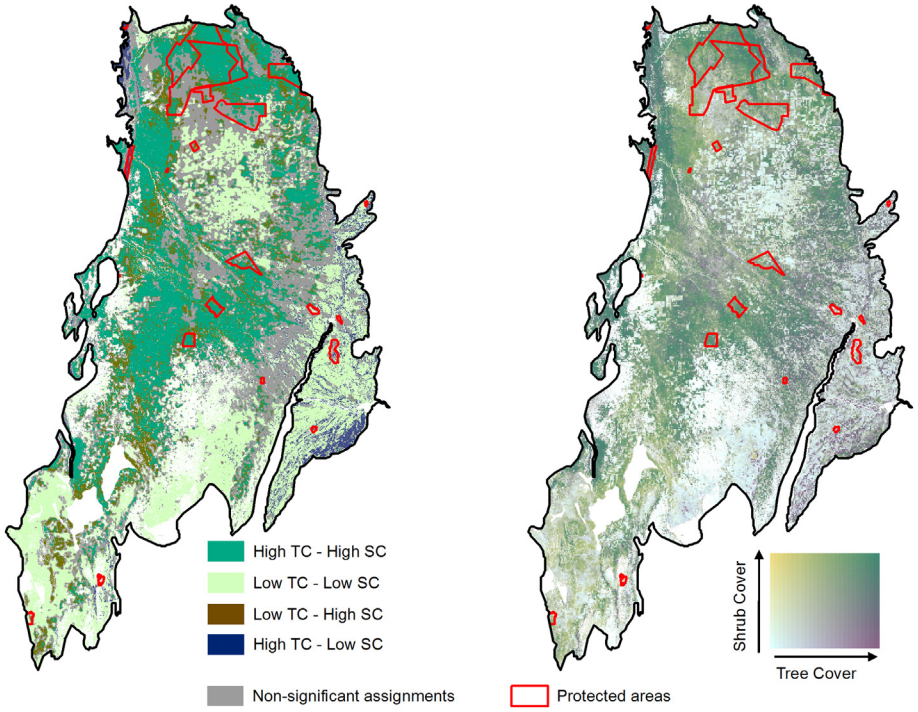

Fig. 5. Left: spatial clusters (high TC/High SC and low SC/low SC) and outliers (low TC/high SC and high TC/low SC) of tree and shrub cover based on a bivariate LISA analysis. Right: overlay of TC and SC.

and savannas globally, most importantly through agricultural expansion, grazing, logging, and fire management, all of which affect woody vegetation structure and composition. Because these changes in turn impact on biodiversity and ecosystem services, monitoring woody vegetation change in these systems is therefore important, yet challenging because of the spectral complexity that gradients in tree, shrub, and grass cover create. Here, we demonstrate how jointly using of Landsat 8 and Sentinel-1 data in a Gradient Boosting framework allows to separate continuous fields of tree and shrub cover across the 1.1 million km^2 Gran Chaco in South America. Our study provides the following key insights. First, differentiating canopy layers in savannas and dry forests based on remote sensing is possible and allows for a better characterization of woody cover structure and composition than categorical information. Second, using Landsat-8 and Sentinel-1 data together improves the mapping of tree- and shrub-cover compared to using data from one of the two sensors only, but also makes the mapping more prone to artefacts from differences in image availability. Third, our tree and shrub cover layers effectively captured a range of land-use effects on woody cover. Fourth, these effects seem to impact the structure of woody vegetation more strongly than environmental factors. More broadly, our results show that realizing the potentials of the growing Landsat and Sentinel archives allows for a better understanding of dry forest and savanna structure, composition, and functioning.

Generally, our models performed well and provided reliable, and separate, estimates of tree and shrub cover, and our work goes thus substantially beyond prior studies mapping fractional woody cover in the Chaco. Woody cover has been mapped there as part of global (Hansen et al., 2013; Sexton et al., 2013), or continental-scale studies (Pengra et al., 2015), but our study is the first to rely on localized training data, fine-tuned for the ecotones that characterize the Chaco. We know of only one fine-scale study, though focusing on a small region at the southern edge of our study area (González-Roglich and Swenson, 2016). Our work is also substantially broader in scope (1.1 million km^2 compared to 50,000 km^2 in that study). Finally, all existing work has lumped woody cover into one category, while we separated continuous fields of tree and shrub cover at the ecoregional scale, to our knowledge for the first time for any dry forest and savanna region.

Our modeling results also showed that jointly using Landsat 8 and Sentinel-1 data improves woody vegetation mapping. This confirms prior work (e.g., Naidoo et al. (2016), but see also Joshi et al. (2016) for a review), but our results add interesting insights. For example, the use of Landsat data (alone or together with Sentinel-1) yielded generally better models for tree cover than for shrub cover. Contrary, when only using Sentinel-1 data, shrub cover showed better model performances than tree cover (Fig. 4). Several factors explain this: first, larger trees in the Chaco have a stronger phenological cycle compared to shrubs (Marco and Páez, 2002). This phenology was picked up stronger by the Landsat metrics than the Sentinel-1 metrics, because more Landsat observations per pixel were available than from Sentinel-1. Many observations are important to describe phenology well (Baumann et al., 2017c; Massey et al., 2017). Second, SAR data are generally better suited than optical data for detecting scattered vegetation such as shrubs (Ryan et al., 2012) and our results confirm this. However, our analyses also show that multi-sensoral approaches are also more prone to artefacts stemming from uneven image availability, particularly in case of Sentinel-1. As especially SAR image availability increases, these issues and artefacts may become less pronounced, but will likely continue to be a challenge when assessing very large areas. Categorical approaches, such as classification approaches or binning the continuous fields we derived, might be useful in such situation to lessen the influence of data acquisition artefacts.

Both measures had lowest uncertainties at high and low values and higher uncertainties in the mid-range value domain, likely a consequence of two factors. First, our training sample was slightly unbalanced towards lower tree and shrub cover, and these samples potentially had a stronger weight during the parameterization phase. This might also explain why our maps displayed higher uncertainty for areas bordering other ecoregions characterized by high tree cover, such as the Yungas, an area likely not well-represented in our (randomly drawn) training and validation dataset. Second, higher uncertainty in the mid-range domain may result from our tree and shrub definition, which

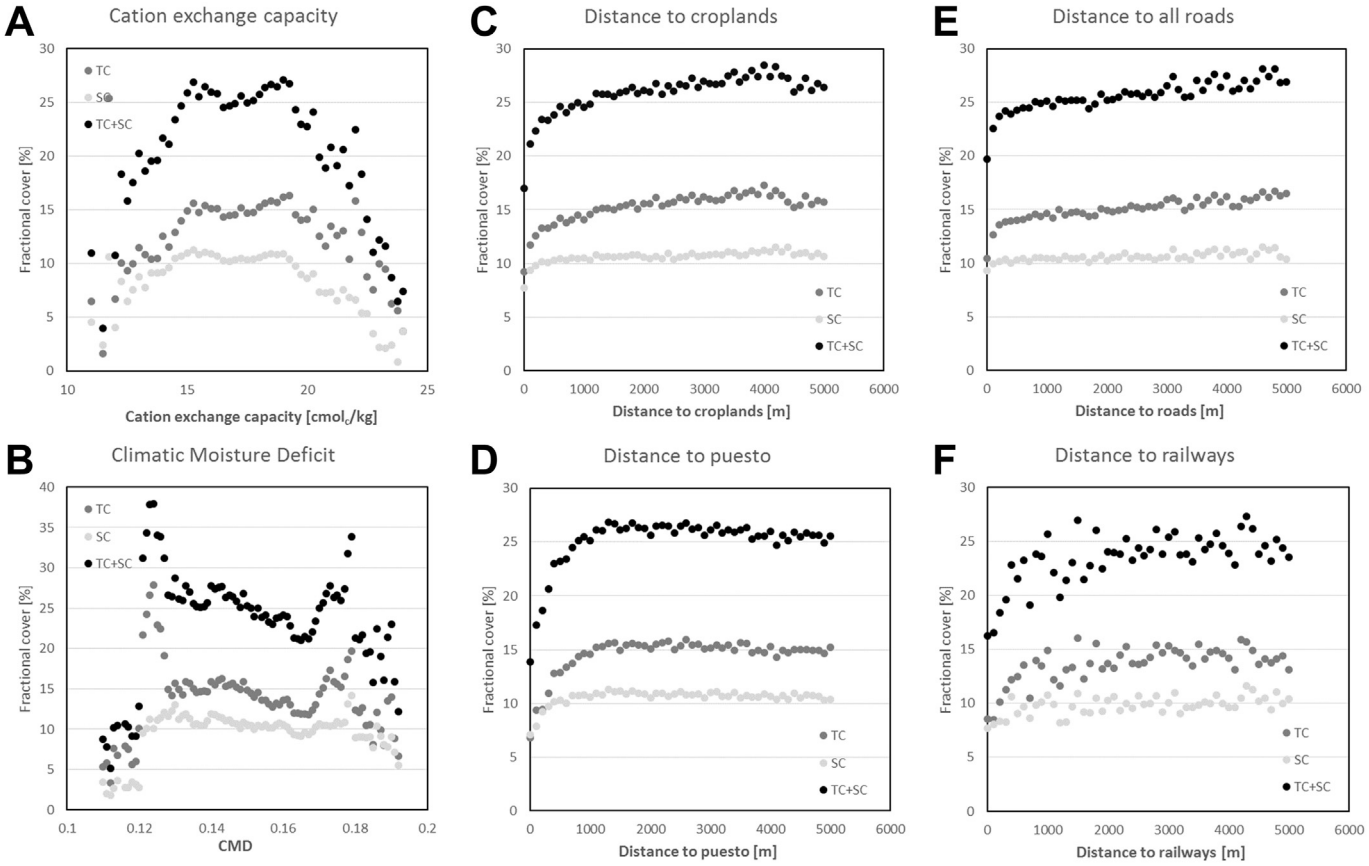

Fig. 6. Average tree cover, shrub cover and overall woody vegetation in relation to (A) cation exchange capacity as a measure for soil quality; (B) Climatic Moisture Deficit representing a climate indicator; (C) distance to croplands; (D) distance to puestos; (E) distance to roads; and (F) distance to railways. Values on the y-axis represent the values for tree cover, shrub cover, and the sum of thereof.

describe a categorization of a continuum of size and structure of woody vegetation, and particularly mid-sized trees may be harder to classify in general, and likely most prevalent where canopies are neither closed nor fully open. Despite remaining uncertainty though, we emphasize the high model performances for both tree and shrub cover and the very similar overall pattern across the different mapping products, providing confidence that the respective layers are a reliable representation of woody vegetation in the Chaco.

Comparing our tree and shrub components to environmental and land-use variables revealed interesting insights into the status and health of Chaco woodlands and savannas. Importantly, our maps highlighted clear, and spatially widespread, effects of certain land-use practices outside woodlands on remaining woody vegetation. For example, cropping had a clear effect on lowering tree and shrub cover closer to fields, likely an effect of pesticide application with airplanes which also spray over surrounding woodlands (Burghardt, 2014), and the use of fire to clear land which may pass over to surrounding forests, comparable to the Amazon (Cochrane and Laurance, 2002). Likewise, smallholders affect woody vegetation substantially surrounding their ranches (i.e., puestos). Impact decreases as cattle cannot roam too far due to water access that is provided at the puesto itself, and because wood collection becomes harder with increasing distance (Gasparri et al., 2010; Macchi and Grau, 2012), and our results reflect these patterns well (Fig. 6). Moreover, our results suggest that infrastructure, such as roads or railways, affects only tree cover, whereas shrub cover remains largely unaffected. This reflects parts of the early land-use history of the Chaco. Between the 1870s and the 1960s/70s, *quebracho* trees were harvested for tannin extraction used during leather production (*quebracho colorado* contains 31% of tannin). Only the largest trees were extracted, and the harvest location was closely connected to the development of the road and railway network (Stunnenberg and Kleinpenning, 1993; Stunnenberg, 1993). As our results show, the Chaco still carries these legacies, as *quebrachos* can take up to hundred until re-grown to full size.

Interestingly, we found all land-use-related factors to shape the structure and composition of dry forests and savannas in the Chaco stronger than biophysical factors. For example, tree cover decreased with increasing CMD, with exception at very high values, which likely represent areas where trees reach the ground water and therefore are less dependent on climatic moisture, likely resulting in the high tree cover values in our map. However, compared to land-use related factors, this trend was substantially weaker, further highlighting the degree of human pressure on the landscape and the urgency to take more action in protecting the remaining forests, as human pressure seems to be a stronger determinant of the forest structure compared to natural constraints.

Our analyses resulted in high model performance, reliable maps, and show highly plausible patterns of tree and shrub cover across the vast Chaco region. Still, some sources of uncertainties and some limitations require mentioning. First, we only used centrality spectral metrics, but did not consider variance-based image metrics. Likewise, we did not consider seasonally-tuned composites due to limited image availability, particularly in the case of the Sentinel-1 data. While both modifications would likely improve model fits even further, these variance metrics and seasonal composites are more prone to outliers, and including them will therefore come at the expense of artefacts in the resulting woody vegetation maps. Second, the nature of our training data collection caused that we omitted below-canopy vegetation, as on-screen digitization only captures the top canopy layer. This may be the reason for the comparatively lower performance of our SAR-based

models. Forest inventory data may provide more insights here, but currently do not exist for the study area as a whole. Third, our land-use variables were only available for a smaller part of the study region, but it is unlikely that for example unmapped puestos in the south of our study region would reveal a different pattern.

Mapping the extent, structure, and condition of savannas and dry forests is important as they are under strong human pressure. Making use of a new generation of optical and SAR sensors enabled us to separate continuous fields of tree and shrub cover across the entire Gran Chaco. Such maps have a range of application. For instance, fractional woody cover is considered an Essential Biodiversity Variable (EBV) (Brummitt et al., 2017; Kissling et al., 2018; Proença et al., 2017). Indeed, in a companion paper we show that biodiversity, in particular bird communities, react strongly and differently along gradients of tree and shrub cover, with clear thresholds of woody cover below which bird communities collapse (Macchi et al., in review). Likewise, aboveground biomass (AGB) in dry forests and savannas varies substantially depending on the fractions of trees and shrubs (Conti et al., 2014; Gasparri et al., 2008), and our approach and our woody cover layers are therefore likely improvements for biomass estimates based on broad-scale AGB interpolation. Moreover, the Chaco is a major deforestation hotspot globally (Vallejos et al., 2015), but our analyses highlighted that there are still larger patches of relatively intact forests. Many of these are not inside protected areas and our map here can serve as a first-order spatial template for identifying forests of particularly conservation concern (e.g., for safeguarding biodiversity or carbon stocks). Finally, next to deforestation, forest degradation is a major threat to the ecological integrity of the Chaco, and our analyses revealed clear association and spatial patterns of certain land uses and woody cover patterns. This opens up avenues for mapping the spatial footprint of degradation, and considering the temporal depth of the Landsat image archives, to reconstruct degradation trends back to the 1980s. More broadly, our work highlights the value of the rich Landsat archive, especially when supplemented by the growing Sentinel-1 record to go beyond categorical approaches to characterize and map woody vegetation in the world's savannas and tropical dry forests.

Acknowledgements

Funding for this research came from the Federal Ministry of Education and Science (BMBF, project PASANOA, 031B0034A), the German Research Foundation (DFG, project KUJ 2458/5-1), and the Belgian Science Policy Office Research Programme for Earth Observation (belspo-STEREO-III, project REFORCHA, SR/00/338). This research contributes to the Landsat Science Team and the Global Land Program (www.glp.earth).

References

Abreu, R.C.R., Hoffmann, W.A., Vasconcelos, H.L., Pilon, N.A., Rossatto, D.R., Durigan, G., 2017. The biodiversity cost of carbon sequestration in tropical savanna. Sci. Adv. 3, e1701284.
Anselin, L., 1995. Local Indicators of Spatial Association—LISA. Geogr. Anal. 27, 93–115.
Anselin, L., Syabri, I., Kho, Y., 2006. GeoDa: an introduction to spatial data analysis. Geogr. Anal. 38, 5–22.
Archer, S., Schimel, D.S., Holland, E.A., 1995. Mechanisms of shrubland expansion - land-use, climate or Co-2. Clim. Chang. 29, 91–99.
Archibald, S., Bond, W.J., Stock, W.D., Fairbanks, D.H.K., 2005. Shaping the landscape: Fire-grazer interactions in an African Savanna. Ecol. Appl. 15, 96–109.
Asner, G.P., Archer, S., Hughes, R.F., Ansley, R.J., Wessman, C.A., 2003. Net changes in regional woody vegetation cover and carbon storage in Texas Drylands, 1937–1999. Glob. Chang. Biol. 9, 316–335.
Baumann, M., Piquer-Rodríguez, M., Fehlenberg, V., Gavier Pizarro, G., Kuemmerle, T., 2016. Land-use competition in the South American Chaco. In: Niewöhner, J., Bruns, A., Hostert, P., Krueger, T., Nielsen, Ø.J., Haberl, H., Lauk, C., Lutz, J., Müller, D. (Eds.), Land Use Competition: Ecological, Economic and Social Perspectives. Cham, Springer International Publishing, pp. 215–229.
Baumann, M., Gasparri, I., Piquer-Rodríguez, M., Gavier Pizarro, G., Griffiths, P., Hostert, P., Kuemmerle, T., 2017a. Carbon emissions from agricultural expansion and intensification in the Chaco. Glob. Chang. Biol. 23, 1902–1916.
Baumann, M., Israel, C., Piquer-Rodríguez, M., Gavier-Pizarro, G., Volante, J.N., Kuemmerle, T., 2017b. Deforestation and cattle expansion in the Paraguayan Chaco 1987–2012. Reg. Environ. Chang. 17, 1179–1191.
Baumann, M., Ozdogan, M., Richardson, A.D., Radeloff, V.C., 2017c. Phenology from Landsat when data is scarce: Using MODIS and Dynamic Time-Warping to combine multi-year Landsat imagery to derive annual phenology curves. Int. J. Appl. Earth Obs. Geoinf. 54, 72–83.
Bleyhl, B., Baumann, M., Griffiths, P., Heidelberg, A., Manvelyan, K., Radeloff, V.C., Zazanashvili, N., Kuemmerle, T., 2017. Assessing landscape connectivity for large mammals in the Caucasus using Landsat 8 seasonal image composites. Remote Sens. Environ. 193, 193–203.
Brandt, M., Hiernaux, P., Tagesson, T., Verger, A., Rasmussen, K., Diouf, A.A., Mbow, C., Mougin, E., Fensholt, R., 2016. Woody plant cover estimation in drylands from Earth Observation based seasonal metrics. Remote Sens. Environ. 172, 28–38.
Brummitt, N., Regan, E.C., Weatherdon, L.V., Martin, C.S., Geijzendorffer, I.R., Rocchini, D., Gavish, Y., Haase, P., Marsh, C.J., Schmeller, D.S., 2017. Taking stock of nature: Essential Biodiversity Variables explained. Biol. Conserv. 213, 252–255.
Bucher, E.H., Huntley, B.J., Walker, B.H., 1982. Chaco and Caatinga — South American Arid Savannas, Woodlands And Thickets. In: Ecology of Tropical Savannas. Berlin, Heidelberg, Springer Berlin Heidelberg, pp. 48–79.
Burghardt, P., 2014. Der Tot kommt mit dem Wind. In: Sueddeutsche Zeitung, . http://sz-magazin.sueddeutsche.de/texte/anzeigen/42435/Der-Tod-kommt-mit-dem-Wind.
Cabido, M., Zeballos, S.R., Zak, M., Carranza, M.L., Giorgis, M.A., Cantero, J.J., Acosta, A.T.R., Paruelo, J., 2018. Native woody vegetation in central Argentina: classification of Chaco and Espinal forests. Appl. Veg. Sci. *21*, 298–311.
Cabrera, A.L., 1976. Regiones Fitogeograficas de Argentina. ACME, Buenos Aires (Argentina).
Carreiras, J.M.B., Jones, J., Lucas, R.M., Shimabukuro, Y.E., 2017. Mapping major land cover types and retrieving the age of secondary forests in the Brazilian Amazon by combining single-date optical and radar remote sensing data. Remote Sens. Environ. *194*, 16–32.
Ceddia, M.G., Zepharovich, E., 2017. Jevons paradox and the loss of natural habitat in the Argentinean Chaco: the impact of the indigenous communities' land titling and the Forest Law in the province of Salta. Land Use Policy 69, 608–617.
Chen, X., Liu, Y.Y., Evans, J.P., Parinussa, R.M., van Dijk, A.I.J.M., Yebra, M., 2018. Estimating fire severity and carbon emissions over Australian tropical savannahs based on passive microwave satellite observations. Int. J. Remote Sens. 1–20.
Chomitz, K., Gray, A.D., 1995. Roads, lands, markets, and deforestation. In: World Bank, Policy Research Department, Environment, Infrastructure, and Agriculture Division.
Cochrane, M.A., Laurance, W.F., 2002. Fire as a large-scale edge effect in Amazonian forests. J. Trop. Ecol. 18, 311–325.
Conti, G., Perez-Harguindeguy, N., Quetier, F., Gorne, L.D., Jaureguiberry, P., Bertone, G.A., Enrico, L., Cuchietti, A., Diaz, S., 2014. Large changes in carbon storage under different land-use regimes in subtropical seasonally dry forests of southern South America. Agric. Ecosyst. Environ. 197, 68–76.
de Carvalho, W.D., Mustin, K., 2017. The highly threatened and little known Amazonian savannahs. 1, 0100.
Defries, R.S., Hansen, M.C., Townshend, J.R.G., 2000. Global continuous fields of vegetation characteristics: a linear mixture model applied to multi-year 8 km AVHRR data. Int. J. Remote Sens. 21, 1389–1414.
Durigan, G., Ratter, J.A., 2006. Successional changes in Cerrado and Cerrado/forest ecotonal vegetation in western Sao Saulo State, Brzil, 1962–2000. Edinb. J. Bot. 63, 119–130.
Elith, J., Leathwick, J.R., Hastie, T., 2008. A working guide to boosted regression trees. J. Anim. Ecol. 77, 802–813.
Espirito-Santos, M.M., Leite, M.E., Silva, J.O., Barbosa, R.S., Rocha, A.M., Anaya, F.C., Dupin, M.G.V., 2016. Understanding patterns of land-cover change in the Brazilian Cerrado from 2000 to 2015. Philos. Trans. R. Soc. B 371.
Friedman, J.H., 2001. Greedy function approximation: a gradient boosting machine. Ann. Stat. 29, 1189–1232.
Gasparri, N.I., Grau, H.R., Manghi, E., 2008. Carbon pools and emissions from deforestation in extra-tropical forests of northern Argentina between 1900 and 2005. Ecosystems 11, 1247–1261.
Gasparri, N.I., Parmuchi, M.G., Bono, J., Karszenbaum, H., Montenegro, C.L., 2010. Assessing multi-temporal Landsat 7 ETM+ images for estimating above-ground biomass in subtropical dry forests of Argentina. J. Arid Environ. 74, 1262–1270.
Gessner, U., Machwitz, M., Conrad, C., Dech, S., 2013. Estimating the fractional cover of growth forms and bare surface in savannas. A multi-resolution approach based on regression tree ensembles. Remote Sens. Environ. 129, 90–102.
Gillespie, T.W., Grijalva, A., Farris, C.N., 2000. Diversity, composition, and structure of tropical dry forests in central America. Plant Ecol. 147, 37–47.
González-Roglich, M., Swenson, J.J., 2016. Tree cover and carbon mapping of Argentine savannas: scaling from field to region. Remote Sens. Environ. 172, 139–147.
Grace, J., San José, J., Meir, P., Miranda, H.S., Montes, R.A., 2006. Productivity and carbon fluxes of tropical savannas. J. Biogeogr. 33, 387–400.
Graesser, J., Aide, M., Grau, R., Ramankutty, N., 2015. Cropland/pastureland dynamics and the slowdown of deforestation in Latin America. Environ. Res. Lett. 10, 034017.
Grau, H.R., Gasparri, N.I., Aide, T.M., 2008. Balancing food production and nature conservation in the Neotropical dry forests of northern Argentina. Glob. Chang. Biol. 14, 985–997.
Griffiths, P., van der Linden, S., Kuemmerle, T., Hostert, P., 2013. A pixel-based Landsat compositing algorithm for large area land cover mapping. IEEE J. Sel. Top. Appl. Earth Observ. Remote Sens. PP, 1–14.
Griffiths, P., Kuemmerle, T., Baumann, M., Radeloff, V.C., Abrudan, I.V., Lieskovsky, J., Munteanu, C., Ostapowicz, K., Hostert, P., 2014. Forest disturbances, forest recovery, and changes in forest types across the Carpathian ecoregion from 1985 to 2010 based on Landsat image composites. Remote Sens. Environ. 151, 72–88.

Hamann, A., Wang, T.L., Spittlehouse, D.L., Murdock, T.Q., 2013. A comprehensive, high-resolution database of historical and projected climate surfaces for western North America. Bull. Am. Meteorol. Soc. 94, 1307–1309.
Hansen, M.C., DeFries, R.S., 2004. Detecting long-term global forest change using continuous fields of tree-cover maps from 8-km advanced very high resolution radiometer (AVHRR) data for the years 1982–99. Ecosystems 7, 695–716.
Hansen, M.C., DeFries, R.S., Townshend, J.R.G., Carroll, M., Dimiceli, C., Sohlberg, R.A., 2003. Global percent tree cover at a spatial resolution of 500 meters: first results of the MODIS Vegetation Continuous Fields algorithm. Earth Interact. 7.
Hansen, M., DeFries, R., Townshend, J.R., Carroll, M., Dimiceli, C., Sohlberg, R., 2006. Vegetation Continuous Fields MOD44B, 2001 Percent Tree Cover, Collection 4. University of Maryland, College Park, Maryland, pp. 2001.
Hansen, M.C., Egorov, A., Roy, D.P., Potapov, P., Ju, J.C., Turubanova, S., Kommareddy, I., Loveland, T.R., 2011. Continuous fields of land cover for the conterminous United States using Landsat data: first results from the web-enabled Landsat data (WELD) project. Remote Sens. Lett. 2, 279–288.
Hansen, M.C., Potapov, P.V., Moore, R., Hancher, M., Turubanova, S.A., Tyukavina, A., Thau, D., Stehman, S.V., Goetz, S.J., Loveland, T.R., Kommareddy, A., Egorov, A., Chini, L., Justice, C.O., Townshend, J.R.G., 2013. High-resolution global maps of 21st-century Forest cover change. Science 342, 850–853.
Hastie, T., Tibshirani, R., Friedman, J., 2009. The Elements of Statistical Learning. Springer, New York.
Hayes, D.J., Cohen, W.B., Sader, S.A., Irwin, D.E., 2008. Estimating proportional change in forest cover as a continuous variable from multi-year MODIS data. Remote Sens. Environ. 112, 735–749.
Higginbottom, T.P., Symeonakis, E., Meyer, H., van der Linden, S., 2018. Mapping fractional woody cover in semi-arid savannahs using multi-seasonal composites from Landsat data. ISPRS J. Photogramm. Remote Sens. 139, 88–102.
House, J.I., Archer, S., Breshears, D.D., Scholes, R.J., 2003. Conundrums in mixed woody-herbaceous plant systems. J. Biogeogr. 30, 1763–1777.
Irons, J.R., Dwyer, J.L., Barsi, J.A., 2012. The next Landsat satellite: the Landsat data continuity mission. Remote Sens. Environ. 122, 11–21.
ISRIC - World Soil Information, 2013. SoilGrids: An Automated System for Global Soil Mapping. Online. ISRIC - World Soil Information, Wageningen, The Netherlands Available. http://www.isric.org/data/soilgrids.
Johansen, K., Phinn, S., 2006. Mapping structural parameters and species composition of riparian vegetation using IKONOS and landsat ETM plus data in Australian tropical savannahs. Photogramm. Eng. Remote. Sens. 72, 71–80.
Joshi, N., Baumann, M., Ehammer, A., Fensholt, R., Grogan, K., Hostert, P., Jepsen, M., Kuemmerle, T., Meyfroidt, P., Mitchard, E., Reiche, J., Ryan, C., Waske, B., 2016. A review of the application of optical and radar remote sensing data fusion to land use mapping and monitoring. Remote Sens. 8, 70.
Kaya, F., Bibi, F., Žliobaitė, I., Eronen, J.T., Hui, T., Fortelius, M., 2018. The rise and fall of the Old World savannah fauna and the origins of the African savannah biome. Nat. Ecol. Evol. 2, 241–246.
Kissling, W.D., Ahumada, J.A., Bowser, A., Fernandez, M., Fernández, N., García, E.A., Guralnick, R.P., Isaac, N.J.B., Kelling, S., Los, W., McRae, L., Mihoub, J.-B., Obst, M., Santamaria, M., Skidmore, A.K., Williams, K.J., Agosti, D., Amariles, D., Arvanitidis, C., Bastin, L., De Leo, F., Egloff, W., Elith, J., Hobern, D., Martin, D., Pereira, H.M., Pesole, G., Peterseil, J., Saarenmaa, H., Schigel, D., Schmeller, D.S., Segata, N., Turak, E., Uhlir, P.F., Wee, B., Hardisty, A.R., 2018. Building Essential Biodiversity Variables (EBVs) of species distribution and abundance at a global scale. Biol. Rev. 93, 600–625.
Klink, C.A., Machado, R.B., 2005. Conservation of the Brazilian Cerrado. Conserv. Biol. 19, 707–713.
Kuemmerle, T., Altrichter, M., Baldi, G., Cabido, M., Camino, M., Cuellar, E., Cuellar, R.L., Decarre, J., Diaz, S., Gasparri, I., Gavier-Pizarro, G., Ginzburg, R., Giordano, A.J., Grau, H.R., Jobbagy, E., Leynaud, G., Macchi, L., Mastrangelo, M., Matteucci, S.D., Noss, A., Paruelo, J., Piquer-Rodriguez, M., Romero-Munoz, A., Semper-Pascual, A., Thompson, J., Torrella, S., Torres, R., Volante, J.N., Yanosky, A., Zak, M., 2017. Forest conservation: remember Gran Chaco. Science 355, 465.
le Polain de Waroux, Y., Baumann, M., Gasparri, N.I., Gavier-Pizarro, G., Godar, J., Kuemmerle, T., Müller, R., Vázquez, F., Volante, J.N., Meyfroidt, P., 2017. Rents, actors, and the expansion of commodity frontiers in the Gran Chaco. Ann. Assoc. Am. Geogr. 1–22.
Lehmann, C.E.R., 2010. Savannas need protection. Science 327, 642–643.
Ley de Proteccion Ambiental de Bosques Nativos, 2007. Ley No 26331, primera seccion. Argentina, 3pags. Available at. http://www.infoleg.gov.ar/infolegInternet/anexos/135000-139999/136125/norma.htm.
Lucas, R.M., Lee, A.C., Armston, J., 2011. Quantifying carbon in savannas: the role of active sensors in measurements of tree structure and biomass. In: Hill, M.J., Hanan, N.P. (Eds.), Ecosystem Function in Savannas: Measurement and Modeling at Landscape to Global Scales. CRC Press, Boca Raton, Florida, pp. 156–174.
Macchi, L., Grau, H.R., 2012. Piospheres in the dry Chaco. Contrasting effects of livestock puestos on forest vegetation and bird communities. J. Arid Environ. 87, 176–187.
Macchi, L., Grau, H.R., Zelaya, P.V., Marinaro, S., 2013. Trade-offs between land use intensity and avian biodiversity in the dry Chaco of Argentina: a tale of two gradients. Agric. Ecosyst. Environ. 174, 11–20.
Macchi, L., Baumann, M., Bluhm, H., Baker, M., Levers, C., Grau, H.C., Kuemmerle, T. Thresholds in bird community composition along gradients of woddy vegetation in the South American Dry Chaco. (In review).
Marco, D.E., Páez, S.A., 2002. Phenology and phylogeny of animal-dispersed plants in a Dry Chaco forest (Argentina). J. Arid Environ. 52, 1–16.
Masek, J.G., Vermote, E.F., Saleous, N.E., Wolfe, R., Hall, F.G., Huemmrich, K.F., Feng, G., Kutler, J., Teng-Kui, L., 2006. A Landsat surface reflectance dataset for North America, 1990–2000. Geosci. Remote Sens. Lett. IEEE 3, 68–72.
Massey, R., Sankey, T.T., Congalton, R.G., Yadav, K., Thenkabail, P.S., Ozdogan, M., Sánchez Meador, A.J., 2017. MODIS phenology-derived, multi-year distribution of conterminous U.S. crop types. Remote Sens. Environ. 198, 490–503.
Mayle, F.E., Langstroth, R.P., Fisher, R.A., Meir, P., 2007. Long-term forest–savannah dynamics in the Bolivian Amazon: implications for conservation. Philos. Trans. R. Soc. B 362, 291.
Melaas, E.K., Sulla-Menashe, D., Gray, J.M., Black, T.A., Morin, T.H., Richardson, A.D., Friedl, M.A., 2016. Multisite analysis of land surface phenology in North American temperate and boreal deciduous forests from Landsat. Remote Sens. Environ. 186, 452–464.
Mitchard, E.T.A., Saatchi, S.S., Lewis, S.L., Feldpausch, T.R., Woodhouse, I.H., Sonké, B., Rowland, C., Meir, P., 2011. Measuring biomass changes due to woody encroachment and deforestation/degradation in a forest–savanna boundary region of central Africa using multi-temporal L-band radar backscatter. Remote Sens. Environ. 115, 2861–2873.
Moreira, A.G., 2000. Effects of fire protection on savanna structure in Central Brazil. J. Biogeogr. 27, 1021–1029.
Morgan, J.A., Milchunas, D.G., LeCain, D.R., West, M., Mosier, A.R., 2007. Carbon dioxide enrichment alters plant community structure and accelerates shrub growth in the shortgrass steppe. Proc. Natl. Acad. Sci. U. S. A. 104, 14724–14729.
Murphy, B.P., Andersen, A.N., Parr, C.L., 2016. The underestimated biodiversity of tropical grassy biomes. Philos. Trans. R. Soc. Lond. Ser. B Biol. Sci. 371.
Naidoo, L., Mathieu, R., Main, R., Wessels, K., Asner, G.P., 2016. L-band Synthetic Aperture Radar imagery performs better than optical datasets at retrieving woody fractional cover in deciduous, dry savannahs. Int. J. Appl. Earth Obs. Geoinf. 52, 54–64.
Ottinger, M., Clauss, K., Kuenzer, C., 2017. Large-scale assessment of coastal aquaculture ponds with Sentinel-1 time series data. Remote Sens. 9, 440.
Parr, C.L., Lehmann, C.E., Bond, W.J., Hoffmann, W.A., Andersen, A.N., 2014. Tropical grassy biomes: misunderstood, neglected, and under threat. Trends Ecol. Evol. 29, 205–213.
Pedregosa, F., Varoquaux, G., Gramfort, A., Michel, V., Thirion, B., Grisel, O., Blondel, M., Prettenhofer, P., Weiss, R., Dubourg, V., Vanderplas, J., Passos, A., Cournapeau, D., Brucher, M., Perrot, M., Duchesnay, E., 2011. Scikit-learn: machine learning in python. J. Mach. Learn. Res. 12, 2825–2830.
Pengra, B., Long, J., Dahal, D., Stehman, S.V., Loveland, T.R., 2015. A global reference database from very high resolution commercial satellite data and methodology for application to Landsat derived 30m continuous field tree cover data. Remote Sens. Environ. 165, 234–248.
Piquer-Rodríguez, M., Butsic, V., Gärtner, P., Macchi, L., Baumann, M., Gavier Pizarro, G., Volante, J., Gasparri, N.I., Kuemmerle, T., 2018. Drivers of agricultural land-use change in the Argentine Pampas and Chaco regions. Appl. Geogr. 91, 111–122.
Polley, H.W., Mayeux, H.S., Johnson, H.B., Tischler, C.R., 1997. Viewpoint: atmospheric CO2, soil water, and shrub/grass ratios on rangelands. J. Range Manag. 50, 278–284.
Potapov, P.V., Turubanova, S.A., Tyukavina, A., Krylov, A.M., McCarty, J.L., Radeloff, V.C., Hansen, M.C., 2015. Eastern Europe's forest cover dynamics from 1985 to 2012 quantified from the full Landsat archive. Remote Sens. Environ. 159, 28–43.
Potere, D., 2008. Horizontal positional accuracy of Google Earth's high-resolution imagery archive. Sensors 8, 7973.
Proença, V., Martin, L.J., Pereira, H.M., Fernandez, M., McRae, L., Belnap, J., Böhm, M., Brummitt, N., García-Moreno, J., Gregory, R.D., Honrado, J.P., Jürgens, N., Opige, M., Schmeller, D.S., Tiago, P., van Swaay, C.A.M., 2017. Global biodiversity monitoring: from data sources to Essential Biodiversity Variables. Biol. Conserv. 213, 256–263.
Ratter, J.A., Ribeiro, J.F., Bridgewater, S., 1997. The Brazilian cerrado vegetation and threats to its biodiversity. Ann. Bot. 80, 223–230.
Reiche, J., Hamunyela, E., Verbesselt, J., Hoekman, D., Herold, M., 2018. Improving near-real time deforestation monitoring in tropical dry forests by combining dense Sentinel-1 time series with Landsat and ALOS-2 PALSAR-2. Remote Sens. Environ. 204, 147–161.
Rejžek, M., Coria, R.D., Kunst, C., Svátek, M., Kvasnica, J., Navall, M., Ledesma, R., Gómez, A., Matula, R., 2017. To chop or not to chop? Tackling shrub encroachment by roller-chopping preserves woody plant diversity and composition in a dry subtropical forest. For. Ecol. Manag. 402, 29–36.
Ridgeway, G., 2007. Generalized Boosted Models: A Guide to the GBM Package. pp. 2007.
Roques, K.G., O'Connor, T.G., Watkinson, A.R., 2001. Dynamics of shrub encroachment in an African savanna: relative influences of fire, herbivory, rainfall and density dependence. J. Appl. Ecol. 38, 268–280.
Roy, D.P., Ju, J., Kline, K., Scaramuzza, P.L., Kovalskyy, V., Hansen, M., Loveland, T.R., Vermote, E., Zhang, C., 2010. Web-enabled Landsat Data (WELD): Landsat ETM+ composited mosaics of the conterminous United States. Remote Sens. Environ. 114, 35–49.
Roy, D.P., Wulder, M.A., Loveland, T.R., Wookcock, C.E., Allen, R.G., Anderson, M.C., Helder, D., Irons, J.R., Johnson, D.M., Kennedy, R., Scambos, T.A., Schaaf, C.B., Schott, J.R., Sheng, Y., Vermote, E.F., Belward, A.S., Bindschadler, R., Cohen, W.B., Gao, F., Hipple, J.D., Hostert, P., Huntington, J., Justice, C.O., Kilic, A., Kovalskyy, V., Lee, Z.P., Lymburner, L., Masek, J.G., McCorkel, J., Shuai, Y., Trezza, R., Vogelmann, J., Wynne, R.H., Zhu, Z., 2014. Landsat-8: science and product vision for terrestrial global change research. Remote Sens. Environ. 145, 154–172.
Rueda, C.V., Baldi, G., Gasparri, I., Jobbágy, E.G., 2015. Charcoal production in the Argentine Dry Chaco: where, how and who? Energy Sustain. Dev. 27, 46–53.
Ryan, C.M., Hill, T., Woollen, E., Ghee, C., Mitchard, E., Cassells, G., Grace, J., Woodhouse, I.H., Williams, M., 2012. Quantifying small-scale deforestation and forest degradation in African woodlands using radar imagery. Glob. Chang. Biol. 18, 243–257.
Sankaran, M., Ratnam, J., Hanan, N., 2008. Woody cover in African savannas: the role of

resources, fire and herbivory. Glob. Ecol. Biogeogr. 17, 236–245.
Santos, J.R., Lacruz, M.S.P., Araujo, L.S., Keil, M., 2002. Savanna and tropical rainforest biomass estimation and spatialization using JERS-1 data. Int. J. Remote Sens. 23, 1217–1229.
Schwieder, M., Leitão, P.J., da Cunha Bustamante, M.M., Ferreira, L.G., Rabe, A., Hostert, P., 2016. Mapping Brazilian savanna vegetation gradients with Landsat time series. Int. J. Appl. Earth Obs. Geoinf. 52, 361–370.
Sexton, J.O., Song, X.P., Feng, M., Noojipady, P., Anand, A., Huang, C.Q., Kim, D.H., Collins, K.M., Channan, S., DiMiceli, C., Townshend, J.R., 2013. Global, 30-m resolution continuous fields of tree cover: Landsat-based rescaling of MODIS Vegetation Continuous Fields with lidar-based estimates of error. Int. J. Digital Earth 6, 427–448.
Stern, M., Quesada, M., Stoner, K.E., 2002. Changes in composition and structure of a tropical dry forest following intermittent cattle grazing. Revista De Biologia Tropical 50, 1021–1034.
Stunnenberg, P.W., 1993. Entitled to Land: The Incorporation of the Paraguayan and Argentinean Gran Chaco and the Spatial Marginalization of the Indian People. Verlag Breitenbach Publishers.
Stunnenberg, P., Kleinpenning, J., 1993. The role of extractive industries in the process of colonization: the case of quebracho exploitation in the Gran Chaco. Tijdschr. Econ. Soc. Geogr. 84, 220–229.
Tian, F., Brandt, M., Liu, Y.Y., Verger, A., Tagesson, T., Diouf, A.A., Rasmussen, K., Mbow, C., Wang, Y., Fensholt, R., 2016. Remote sensing of vegetation dynamics in drylands: evaluating vegetation optical depth (VOD) using AVHRR NDVI and in situ green biomass data over west African Sahel. Remote Sens. Environ. 177, 265–276.
USGS, 2015. Landsat surface reflectance high level data products. available online. http://landsat.usgs.gov/CDR_LSR.php (last access 1/7/2016).
Vallejos, M., Volante, J.N., Mosciaro, M.J., Vale, L.M., Bustamante, M.L., Paruelo, J.M., 2015. Transformation dynamics of the natural cover in the Dry Chaco ecoregion: a plot level geo-database from 1976 to 2012. J. Arid Environ. 123, 3–11.
Wulder, M.A., Masek, J.G., Cohen, W.B., Loveland, T.R., Woodcock, C.E., 2012. Opening the archive: how free data has enabled the science and monitoring promise of Landsat. Remote Sens. Environ. 122, 2–10.
Zhu, Z., Woodcock, C.E., 2012. Object-based cloud and cloud shadow detection in Landsat imagery. Remote Sens. Environ. 118, 83–94.